

## Evaluation of multi-lane transverse reduction factor under random vehicle load

Xiaoyan Yang<sup>1a</sup>, Jinxin Gong<sup>\*1</sup>, Bohan Xu<sup>1b</sup> and Jichao Zhu<sup>2c</sup>

<sup>1</sup>Department of Civil Engineering, Dalian University of Technology, Dalian, 116023, Liaoning, China

<sup>2</sup>School of Civil Safety Engineering, Dalian Jiaotong University of Technology, 116028, Dalian, China

(Received October 31, 2015, Revised March 7, 2017, Accepted March 9, 2017)

**Abstract.** This paper presents the two-, three-, and four-lane transverse reduction factor based on FEA method, probability theory, and the recently actual traffic flow data. A total of 72 composite girder bridges with various spans, number of lanes, loading mode, and bridge type are analyzed with time-varying static load FEA method by ANSYS, and the probability models of vehicle load effects at arbitrary-time point are developed. Based on these probability models, in accordance to the principle of the same exceeding probability, the multi-lane transverse reduction factor and the span of bridge are determined. Finally, the multi-lane transverse reduction factor obtained is compared with those from AASHTO LRFD, BS5400, JTG D60 or Eurocode. The results show that the vehicle load effect at arbitrary-time point follows lognormal distribution. The two-, three-, and four-lane transverse reduction factors calculated by using FEA method and probability respectively range between 0.781 and 1.027, 0.616 and 0.795, 0.468 and 0.645. Furthermore, a correlation between the FEA and AASHTO LRFD, BS5400, JTG D60 or Eurocode transverse reduction factors is made for composite girder bridges. For the two-, three-, and four-lane bridge cases, the Eurocode code underestimated the FEA transverse reduction factors by 27%, 25% and 13%, respectively. This underestimation is more pronounced in short-span bridges. The AASHTO LRFD, BS5400 and JTG D60 codes overestimated the FEA transverse reduction factors. The FEA results highlight the importance of considering span length in determining the multi-lane transverse reduction factors when designing two-lane or more composite girder bridges. This paper will assist bridge engineers in quantifying the adjustment factors used in analyzing and designing multi-lane composite girder bridges.

**Keywords:** highway bridge; transverse reduction factor; composite girders bridge; random vehicle load; probabilistic model

### 1. Introduction

Composite girder bridges remain one of the most common types of bridges built in many countries. Due to the presence of the bridge deck slab in the superstructure, the live loads are not applied directly to the beams. The concept of the transverse reduction factor allows the design engineer to consider the transverse effect of vehicle loads in determining the moments of beams under vehicle loads, thus simplifying the analysis and design of bridges. According to the approach of the load distribution, maximum moments in beams are obtained first as if the vehicle loads are applied directly to beams. These values are then multiplied by the appropriate transverse reduction factors to obtain critical vehicle-load moments of beams in

bridges. Currently, the transverse reduction factor of the vehicle load moment in highway bridge design is commonly determined using the method in the JTG D60 specification (2015), AASHTO LRFD Specification (2012), AASHTO Standard Specification (2002), British Standard (BS5400 2006, Dawe 2003) or Eurocode Specification (2003). JTG D60 (2015) specification assumed that the loading of vehicle load in each lane is not related. The relation between transverse reduction factor and Annual Average Daily Traffic (AADT)  $Q$  of single lane, number of lanes  $m$  and the design reference period  $T$  of structure is established by the theory on probability of random event in independent repeated trials. The expression of multi-lane transverse reduction factor is obtained (Bao *et al.* 1995, Zhang 2001). The transverse reduction factor of three-lane and four-lane is 0.78 and 0.67, respectively. AASHTO LRFD Specification (2012) assumed that the vehicle load on bridge is under one-way traffic; the AADT of single lane  $Q$  is equal to 5000; the design reference period  $T$  is equal to 75 year; and that the most unfavorable position of vehicle load is loaded to the influence surface of a load effect on the calculated section of structure. The transverse reduction factor of three-lane and four-lane is 0.85 and 0.65, respectively. AASHTO Standard Specification (2002) that results obtained from analyses of three- and four-lane bridge decks where all lanes are loaded simultaneously are

\*Corresponding author, Professor  
E-mail: [jinxingong2012@gmail.com](mailto:jinxingong2012@gmail.com)

<sup>a</sup>Ph.D.  
E-mail: [yangxiaoyan0024@126.com](mailto:yangxiaoyan0024@126.com)

<sup>b</sup>Associate professor  
E-mail: [bohanxu@dlut.edu.cn](mailto:bohanxu@dlut.edu.cn)

<sup>c</sup>Lecturer  
E-mail: [zjc@djtu.edu.cn](mailto:zjc@djtu.edu.cn)

to be multiplied by 0.90 and 0.75, respectively. British Standard (BS5400 2006) and Eurocode specifications (2003) adopts the form of loading a given load in terms of multi-lane transverse reduction. In BS5400, HA load (composed by uniformly distributed load and concentrated load) loaded on two notional lanes, and 1/3 HA load loaded on the other lanes. The calculation results show that the transverse reduction factor of three-lane and four-lane is 0.78 and 0.67, respectively. Eurocode divides the lane into four grades according to the most unfavorable lane of action, and numbers them as ①, ②, ③ and ④. Wherein, ① is the most unfavorable lane, which is followed by ② and ③; ④ refers to other lanes. The lanes in different grades have different grade of loading. The analysis results show that the transverse reduction factor of three-lane and four-lane is 0.52 and 0.46, respectively. It can be seen from the above that the multi-lane transverse reduction factors specified by China, the US and the UK are quite different; this may be caused by incomplete factors considered in determining transverse reduction factor. For example, the probability model of truck load adopted by JTG D60 was obtained through the statistical analysis on actually measured vehicle load in 1980s for Canadian. The vehicle condition in China is not involved. Moreover, the interaction of abutting lane is not considered. AASHTO LRFD specification while considering the relationship of abutting lane, but load effect is calculated by static method, and without considering the randomness of vehicle load. Eurocode adopts the fixed load model, and the influence of actual traffic flow is not considered. All these specifications do not consider the influence of bridge span and bridge type. Therefore, it is necessary to make a further study on multi-lane transverse reduction factor.

At present, many scholars in domestic and abroad have studied the transverse reduction factor of multi-lane bridge from different angles. Meski *et al.* (2011) presented static calculation for one- and two-span reinforced concrete beam-slab bridges with different spans, different beam spacing and different live-loading methods by FEA method. The vehicle load effect of corresponding condition is obtained. Through the comparison with load effect specified by AASHTO Standard (2002), it can be found that the load effect calculated as per specification for bridge with span  $L < 12$  m is conservative. Moreover, through the comparison and the analysis of vehicle load effects calculated by different live-loading methods, it can be obtained that multi-lane transverse reduction factor is related to bridge span and boundary beam. The publications (Mabsout *et al.* 1999, Mabsout *et al.* 2002, Hołowaty 2012) presented the parametric investigation on transverse distribution factor using the three-dimensional (3D) finite-element analysis (FEA) of one- and two-span steel girder bridges. HS20 load (AASHTO LRFD 2012) is loaded to all lanes and part of lanes on bridge structure with different spans and different beam spacing. The static calculation is conducted by 3D FEA method. Mabsout *et al.* (2002) compares the distribution factor by finite element analysis (FEA-DF) with the transverse distribution factor (DF) calculated as per AASHTO Standard (2002) and the Mabsout *et al.* (1997). The results show that the FEA-DF is similar to the result

calculated as per NCHRP. When bridge span  $L > 13.5$  m and the beam spacing is 3 m-3.6 m, FEA-DF is similar to the result calculated as per AASHTO. Mabsout *et al.* (1999) compared the transverse distribution factors after multi-lane reduction, which are obtained through loading HS20 load to part of lanes and loading HS20 load to all lanes, respectively. The results show that the multi-lane transverse reduction factor specified by AASHTO is relatively conservative when bridge span  $> 18.3$  m and girder spacing  $> 1.83$  m. To sum up, multi-lane transverse reduction factor is related to bridge span, and the variation trend that it changes with bridge span is given. However, in finite element calculation, fixed form of vehicle load is loaded to bridge structure, and static calculation is conducted based on this. The randomness of vehicle load is not considered. Moreover, the expression of multi-lane transverse reduction factor and bridge span is not given.

This paper builds on the results reported in the literature and explores in more detail a parametric study of multi-lane distribution in one-span, two-equal-span, bridge width, span length, shoulder width, straight composite girder bridges. Firstly, based on measured data of vehicle load in main road of China, this paper presents the probability model of random vehicle load. The finite element models of composite girder bridges under 72 different conditions are established by ANSYS. The lane load or random vehicle load are applied to the one- and two-span composite girder bridges structure of two-lane, three-lane and four-lane in the forms of loading to single lanes and loading to all lanes. The finite element calculation of time-varying static load is conducted. The probability distribution of vehicle load effect at time-point is put forward. Secondly, the relationship between the multi-lane transverse reduction factors and span lengths are established with the same guaranteed rate based on the probability model of vehicle load effects. Finally, the calculated multi-lane transverse reduction factor is compared to the specified by the specification.

## 2. Bridge model

The publications (Tarhini and Frederick 1992, Mabsout and Jabakhanji 2004) reported a parametric study that showed the bridge deck construction, sectional dimension of support beam, presence of cross bracing, and variation in concrete slab thickness had negligible effect on the transverse reduction factors. Therefore, this study considered span length, slab width, and vehicle-loading condition as the major bridge parameters affecting the multi-lane transverse reduction factor for bending moment in composite girder bridges.

Typical one-span, two-equal-span, two-, three-, and four-lane composite girder bridges are selected for this study. The various lengths considered for the one-span bridges were 10.5, 17.1, 30.3, and 42.9 m (34, 56, 99, and 141 ft), respectively. The overall total span lengths of two-equal-span bridges in this study were 56.1, 69.3, 82.5, and 95.7 m (184, 227, 270, and 314 ft), respectively. The overall bridge width was selected to be a constant 9.15 m (30 ft) for two lanes, 12.81 m (42 ft) for three lanes, and 16.47 m (54

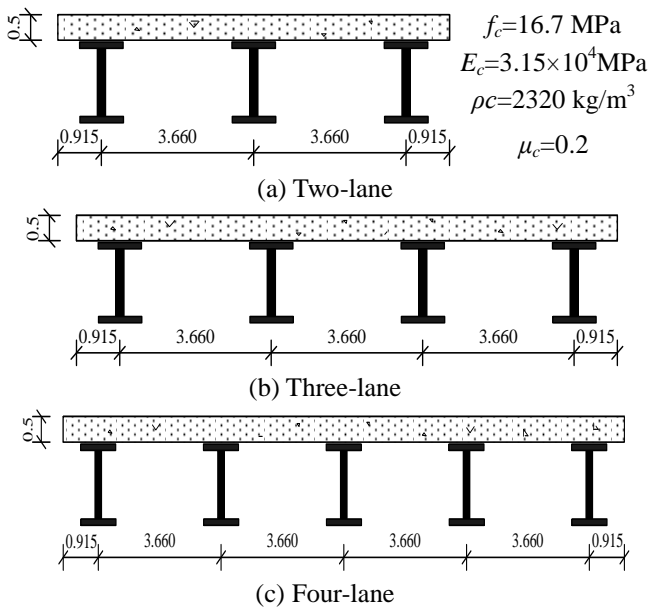


Fig. 1 Cross section of composite girder bridges of two-lane, three-lane and four-lane (unit: m)

ft) for four lanes. The shoulder width on two sides of bridge was 0.915 m (3 ft). All the bridges were non-skewed and had straight beams. The bridge deck cross section consisted of a constant thickness of 500 mm (19.7 in) reinforced concrete slab supported by structural steel girder H1016×1880×140×152 mm spaced at 3.66 m (12 ft), as shown in Fig. 1 for two lanes, three lanes and four lanes.

The material properties used in modeling the highway bridges were normal-strength reinforced and concrete (JTG D62 2004). The compressive strength of the concrete  $f_c$  was 16.7 MPa (4500 psi), the modulus of elasticity  $E_c$  was  $3.15 \times 10^4$  MPa, the density  $\rho_c$  was 2320 kg/m<sup>3</sup>, and the Poisson's ratio  $\mu_c$  was 0.2. The modulus of elasticity of the grade HRB335 reinforcing steel  $E_y$  was  $2.0 \times 10^5$  MPa, the density  $\rho_y$  was 7900 kg/m<sup>3</sup>, and the Poisson's ratio  $\mu_y$  was 0.3.

### 3. Bridge load

#### 3.1 Lane load

General Code for Design of Highway Bridges and Culverts specifies (JTG D60 2015) that the overall calculation of bridge structures adopt lane load which is composed by uniformly distributed load (UDL) and concentrated load (CL). The characteristic value of uniformly distributed load of Grade I highway is  $q_k=10.5$  kN/m. It shall be fully distributed in the same sign influence line which will generate the most unfavorable effect to the structure. The concentrated load  $P_k$  of bridge with different spans is given by the following Eq. (1).

$$P_k(L) = \begin{cases} 180 & L \leq 5\text{m} \\ 4L+160 & 5\text{m} < L < 50\text{m, kN} \\ 360 & L \geq 50\text{m} \end{cases} \quad (1)$$

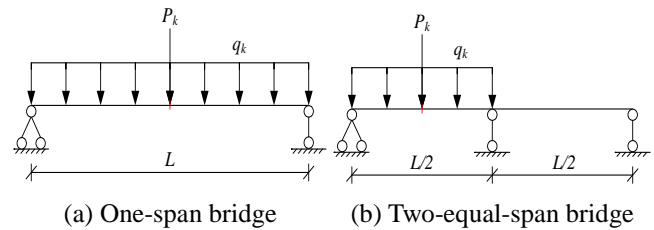


Fig. 2 The most adverse lane load arrangement of mid-span moment

Table 1 Proportion of different types of vehicles

Lane division	Percentage of vehicle types					
	Two-Axle cars	Two-Axle buses	Two-Axle trucks	Tri-Axle trucks	Four-Axle trucks	Five-Axle trucks
Fast lane	74.47	6.32	9.90	2.39	2.68	4.24
Middle lane	57.41	10.79	12.98	7.38	6.47	4.97
Slow lane	52.32	6.42	15.97	9.58	8.33	7.38

where  $P_k$  is the characteristic value of concentrated load (kN), which is arranged in the maximum influence line peak of corresponding influence line;  $q_k$  is the characteristic value of uniformly distributed load (kN/m).  $L$  is the span length of one-span bridges or the total span length of two-equal-span bridges (m). The calculation of Grade I highway lane load arranged as per the most unfavorable position is as shown in Fig. 2.

#### 3.2 Random vehicle load

The bridge loading model is very closely related to gross vehicle weight, axle load and inter-vehicle spacing. In addition, the number and position of wheels changed with time as vehicle moves on a bridge (Mei *et al.* 2004, Gao *et al.* 2008, Helmi *et al.* 2014, Ting *et al.* 2015). That is to say, the gross vehicle weight, axle load and inter-vehicle spacing are all the random variables. Thus, the load effect under vehicle load is a stochastic process. Weighing vehicles as they travel on highways is known as Weigh-in-Motion (WIM) technology. By using a WIM system, virtually a 100% sample of traffic data for statistical purposes can be obtained. The information can be transmitted immediately in real time, or at some future time, to locations remote from the WIM site via conventional communications networks (Miao and Chan 2002). Thus, WIM systems were used to provide a great amount of traffic flow data in this study.

These data were then used to determine the mathematical distributions and statistical parameters of the bridge random vehicle load.

The maximum likelihood estimation approach is adopted to fit traffic flow data recorded by WIM systems. Then, the obtained statistical parameters such as mean value and standard deviation, etc. are verified by Kolmogorov-Smirnov (K-S) test method (Miao and Chan 2002). Because the WIM systems could not record all possible traffic situations, Monte-Carlo simulation was used to regenerate traffic records for any chosen scenario.

#### (1) Proportion of different types of vehicles

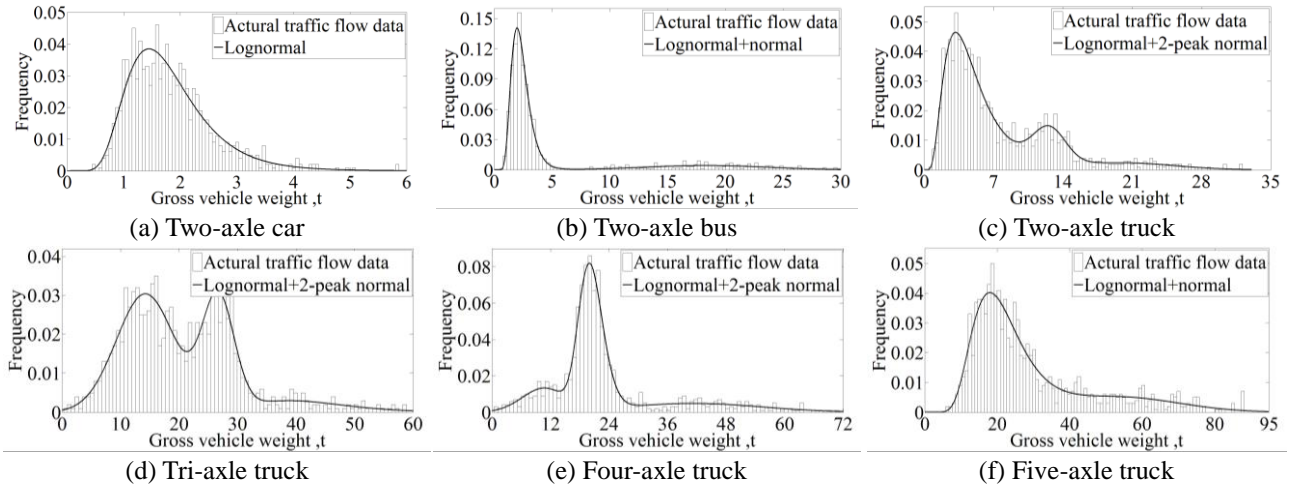


Fig. 3 Fitted probability density curve of different types of vehicle loads in fast lane

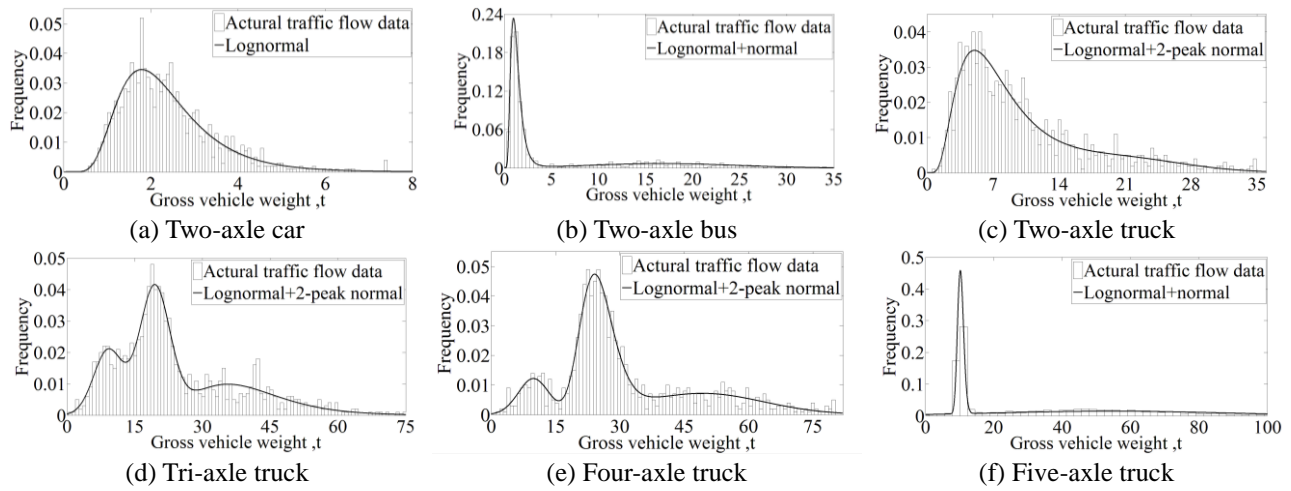


Fig. 4 Fitted probability density curve of different types of vehicle loads in middle lane

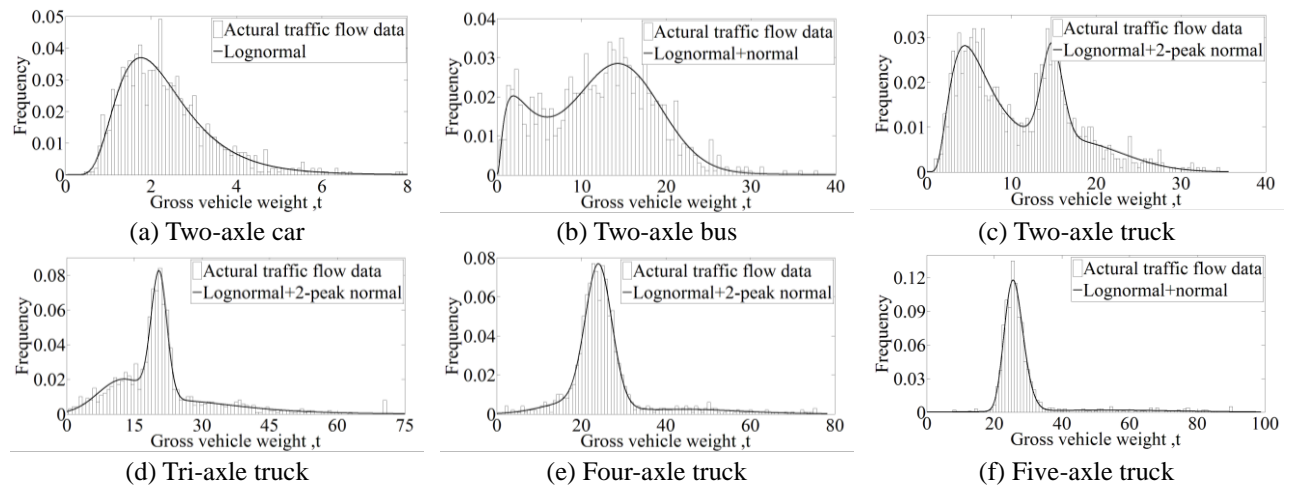


Fig. 5 Fitted probability density curve of different types of vehicle loads in slow lane

The proportion of different types of vehicles in fast lane (left lane), middle lane and slow lane (right lane) can be obtained by statistical analysis of the actual traffic flow, as shown in Table 1.

(2) Gross vehicle weights

When statistical analysis is conducted for the probability distribution of gross vehicle weight, the following basic assumptions shall be met: (1) A certain section of bridge is under the single action of vehicle load, and the influence of other factors is not considered. (2) The operating state of

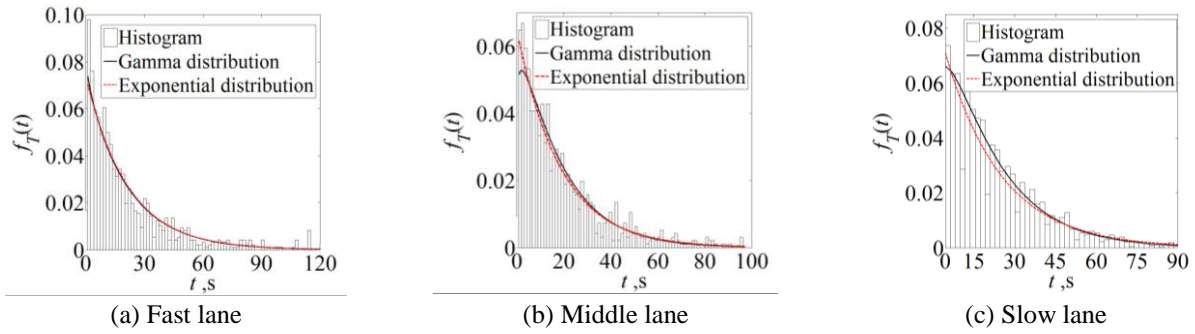


Fig. 6 Statistical analysis of vehicle time-interval

Table 2 Statistical parameter of gross vehicle weight

Lane division	Vehicle types	$P_1$	$\mu_{lnX1}$	$\sigma_{lnX1}$	$P_2$	$\mu_{X2}, t$	$\sigma_{lnX2}, t$	$P_3$	$\mu_{X3}, t$	$\sigma_{lnX3}, t$
Fast lane	Two-Axle car	1.000	0.538	0.410	—	—	—	—	—	—
	Two-Axle bus	0.822	0.793	0.350	0.178	18.535	5.183	—	—	—
	Two-Axle truck	0.744	1.425	0.543	0.164	11.992	1.999	0.091	19.918	5.037
	Tri-Axle truck	0.111	3.624	0.259	0.611	14.041	5.327	0.279	26.561	2.539
	Four-Axle truck	0.634	3.003	0.124	0.213	40.342	15.572	0.153	10.630	4.329
Middle lane	Two-Axle car	1.000	0.772	0.442	—	—	—	—	—	—
	Two-Axle bus	0.672	0.174	0.434	0.328	16.427	7.261	—	—	—
	Two-Axle truck	0.836	1.994	0.567	0.164	20.753	7.689	—	—	—
	Tri-Axle truck	0.337	3.616	0.295	0.196	8.567	3.027	0.467	18.788	3.577
	Four-Axle truck	0.542	3.206	0.159	0.309	47.974	14.375	0.150	10.164	3.651
Slow lane	Two-Axle car	1.000	0.627	0.419	—	—	—	—	—	—
	Two-Axle bus	0.240	1.485	0.930	0.760	14.057	5.435	—	—	—
	Two-Axle truck	0.562	1.856	0.589	0.194	14.775	1.284	0.243	17.205	6.208
	Tri-Axle truck	0.192	3.467	0.340	0.421	13.519	6.280	0.387	20.485	1.829
	Four-Axle truck	0.106	3.898	0.230	0.182	20.978	8.233	0.712	23.908	3.016

vehicle load in fast lane, middle lane and slow lane is considered, respectively. (3) The vehicle load and the interval of vehicle load in each lane are independent and identically distributed random variables. The stochastic process of vehicle load and number of vehicle is independent.

The gross vehicle weights of two-axle cars obey the lognormal distribution, and the probability density function is given by

$$f_X(x) = \frac{1}{\sqrt{2\pi}\sigma_{\ln X_1} x} \exp\left[-\frac{1}{2}\left(\frac{\ln(x) - \mu_{\ln X_1}}{\sigma_{\ln X_1}}\right)^2\right] \quad (2)$$

where,  $X$  is the random variable of vehicle load ( $t$ ),  $\mu_{\ln X_1}$ ,  $\sigma_{\ln X_1}$  are respectively the mean and standard deviation of the logarithm of the two-axle car, as shown in Table 2.

A multi-peak distribution with two or three peaks, consists of a weighted sum of lognormal distribution and normal distributions, which can appropriately describe the gross vehicle weight of two-axle buses, two-, tri-, four-,

five-axle trucks. The multi-peak probability density function is given by

$$f_X(x) = \frac{p_1}{\sigma_{\ln X_1} x} \varphi\left(\frac{\ln(x) - \mu_{\ln X_1}}{\sigma_{\ln X_1}}\right) + \sum_{i=2}^n \frac{p_i}{\sigma_{X_i}} \varphi\left(\frac{x - \mu_{X_i}}{\sigma_{X_i}}\right) \quad \sum_{i=1}^n p_i = 1 \quad (3)$$

where  $p_1$  is the proportion of the 1st overall vehicle load;  $p_i$  is the proportion of the  $i$  th overall vehicle load;  $\mu_{\ln X_1}$ ,  $\sigma_{\ln X_1}$  are respectively the mean and standard deviation of the logarithm of the 1 th overall vehicle load, as shown in Table 2;  $\mu_{X_i}$ ,  $\sigma_{X_i}$  are respectively the mean and standard deviation of the  $i$  th overall vehicle load ( $t$ ), as shown in Table 2;  $\varphi(\cdot)$  is the probability density function of the standard normal random variable.

Figs. 3-5 illustrate the statistical histograms of the gross vehicle weights of different types of vehicles and their fitted theoretical distributions.

### (3) Time-interval of vehicle

The statistical analysis is also carried out to determine time-interval in vehicle load model. According to measured data of traffic flow, the histograms of the acquired data are shown in Fig. 6. Gamma distribution and exponential distribution are to be merged for K-S test, and confidence level  $\alpha=0.05$  is taken. The result shows that time-interval of vehicle does not refuse to obey gamma distribution and exponential distribution.

Probability density function of gamma distribution is as follows

$$f_T(t) = \frac{b^a}{\Gamma(a)} t^{a-1} e^{-bt} \quad (4)$$

where  $t$  is the random variable of time-interval of vehicle ( $s$ );  $\Gamma(\cdot)$  is gamma function;  $a$  and  $b$  are parameters.

Probability density function of exponential distribution is as follows

$$f_T(t) = \lambda e^{-\lambda t} \quad (5)$$

where  $\lambda$  is parameter.

## 4. Calculation and analysis of finite element

### 4.1 Finite element model

The geometry of a bridge superstructure can be idealized for theoretical analysis in many ways. The

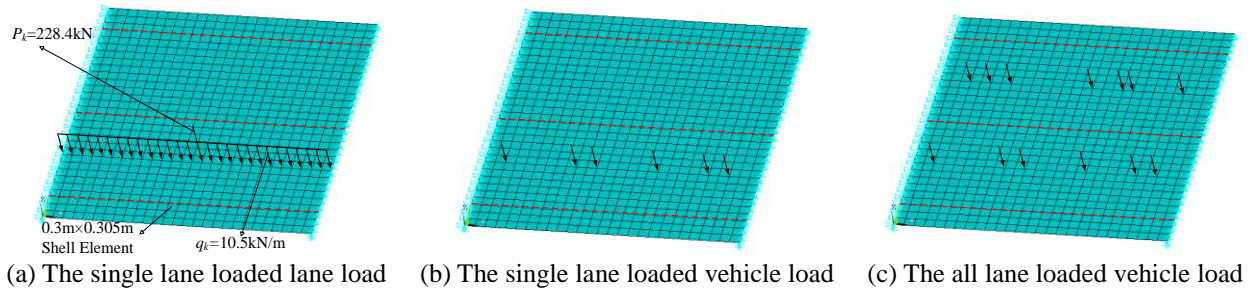


Fig. 8 Schematic diagram for lane load and vehicle load at arbitrary-time point for one-span, two-lane bridges

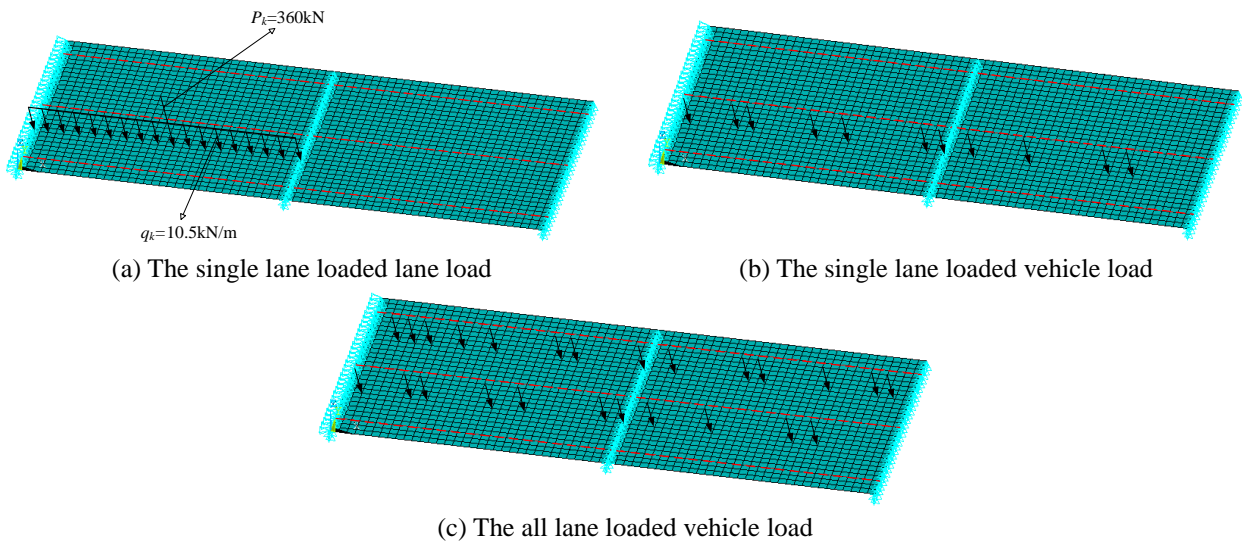


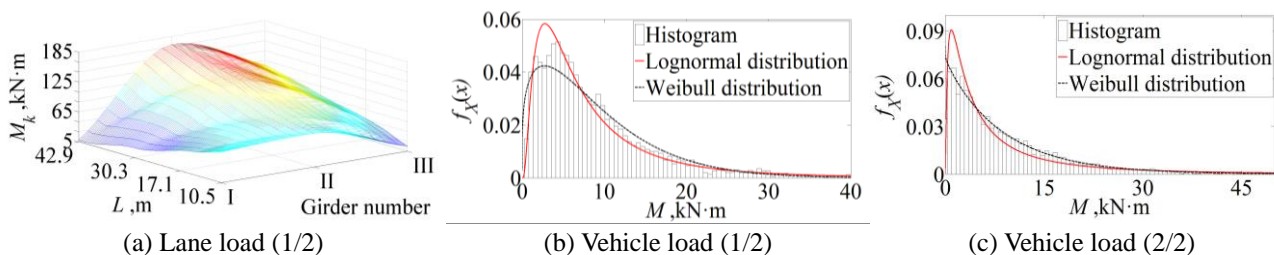
Fig. 9 Schematic diagram for lane load and vehicle load at arbitrary-time point for two-equal-span, two-lane bridges

various assumptions and simplifications used in formulating and idealizing the bridge superstructure can have a significant effect on how closely the calculated results match the actual behavior. The finite-element method can be used to predict the actual behavior of complex structures. Bridge superstructures can be modeled using FEA in many ways. It is in the idealization phase of the analysis—the selection of the finite-element models that the greatest differences in approaches are encountered (Frederick and Tarhini 2000, Mabsout *et al.* 1997, Patrick and Huo 2004). Generally, the concrete slab is simplified into idealized quadrilateral shell element, space steel girder is simplified into idealized beam element, the centroid of space steel girders and concrete slab are in the same plane. The simplification can accurately simulate complex bridge structure and vehicle position on the bridge deck. Therefore, this paper builds finite element model of composite girder bridges through finite element program ANSYS. All elements of the finite-element models are considered to be linear elastic, and small deformations and deflections are assumed in the process of analysis. The concrete slabs are modeled using quadrilateral shell elements, SHELL63, with six degrees of freedom at each node. The steel girders are idealized as space-frame beam members, BEAM44, with six degrees of freedom at each node. A typical square-element size of  $0.3 \times 0.305$  m ( $1 \times 1$  ft) is tested and adopted for the concrete slab discretization.

The centroid of all steel girders coincides with the centroid of concrete slab elements. Hinges and rollers are assigned at bearing locations to simulate one-span boundary conditions (Altunişik *et al.* 2013).

#### 4.2 Bridge loading

For multilane loading, the vehicle load per lane is reduced to account for the reduced probability of several lanes being loaded simultaneously by vehicles. The reduced per-lane loading is a scaled-down version of the loading specified for single-lane loading. The primary loading for most major highways are the lane truck loading or the random vehicle loading. Thus, the load is applied to bridge structure through three load modes: (1) The lane load by *General Code for Design of Highway Bridges and Culverts* (JTG D60 2015) is placed in one out of two lanes, one out of three lanes, and one out of four lanes; (2) According to random vehicle load model in section 3.2, a group of random vehicle loads is generated through Monte-Carlo method, on the assumption that the vehicle loads are traveling in the same direction and then is placed in one out of two lanes, one out of three lanes, and one out of four lanes; (3) According to random vehicle load model in section 3.2,  $c$  groups of random vehicle loads are generated through Monte-Carlo method, wherein,  $c$  represents the number of lanes, and then are placed in full lanes. The transverse vehicle load position is considered center in its



\* $M_k$  is characteristic value of lane load effect (kN·m); 1/2 (1/3, 1/4) represents loaded vehicle loads on one out of two lane, one out of three land, and one out of four lane bridges structures; 2/2 (3/3, 4/4) represents loaded vehicle loads on all lanes of bridges structures

Fig. 10 The bending moment of mid-span section in  $L=17.1$ , one-span, two-lane bridge

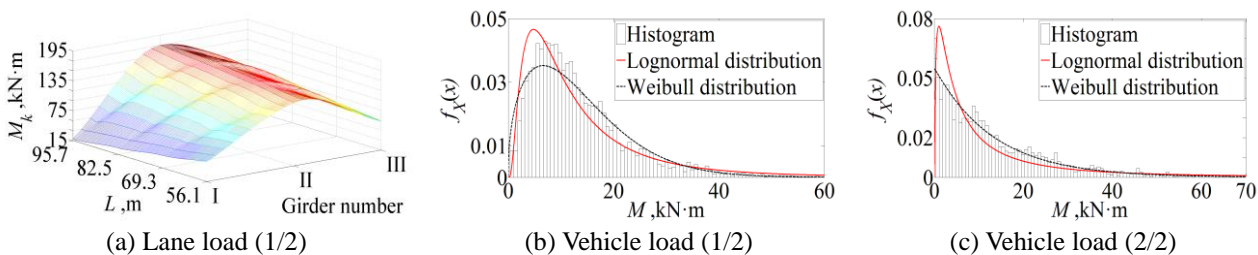


Fig. 11 The bending moment of mid-span section in  $L=69.3$  m, two-equal-span, two-lane bridge

own lane as prescribed. Compared with girder spacing, mesh size of concrete slab is smaller, lane load or vehicle load can be approximately considered to be loaded on element node of deck slab. The typical one out of two lanes loaded for one-span,  $L=17.1$  m and two-equal-span,  $L=69.3$  m composite girder bridges are shown in Figs. 8-9.

### 4.3 Calculation and analysis of vehicle load effect

The single-beam bending moment (load effect) is calculated using JTG D60 lane load or random vehicle load positioned on the beam to produce the maximum bending moment. The maximum girder moments in the bridge superstructure are calculated using the general computer program ANSYS. A total of 72 distinct bridge cases are modeled using 3D finite-element analysis subject to time-varying static loading.

The bending moment of beam element at longitudinal mid-span or near mid-span is used to determine mid-span section moment of composite girder bridges. As shown in Figs. 10(a) and 11(a), the mid-span section moment of composite girder bridges could be determined when lane load is applied on one out of two lane bridge structures. Mid-span section moment of steel girders I decreases with increase of bridge span, and mid-span section moments of steel girders II and III increases with increase of bridge span. The increase amplitude for mid-span section moment of steel girders II is the largest. Therefore, mid-span section moment of steel girders II is suggested as the vehicle load effect sample value in this paper.

According to random vehicle load model developed in section 3.2, random vehicle load obtained by Monte-Carlo method is applied to single lane (1/2, 1/3, 1/4) and all the lanes (2/2, 3/3, 4/4) in the same bridge structure, respectively. It is assumed that the vehicles would move slow enough so as not to produce any dynamic or impact

effects. Thus, random vehicle moves along the longitudinal direction on the bridge with 0.3 m step size and then the vehicle load effect of mid-span section of steel girder II at arbitrary-time point is extracted. Figs. 10(b), 11(b), 10(c) and 11(c) indicates that statistical histogram for vehicle load effect of mid-span section in steel girder II when random vehicle load is loaded to one out of two lane (1/2) and all lanes (2/2) to one- and two-span bridge structure.

For sample value of vehicle load effects generated by random vehicle load in Section 3.2. Fitting testing is made for Weibull distribution and lognormal distribution with K-S test and significance level  $\alpha=0.05$  is taken. Through testing: significance level of Weibull distribution is 0.442; significance level of lognormal distribution is 0.457. Therefore, we can believe that vehicle load effect does not refuse to obey Weibull distribution and lognormal distribution. It is evident from Figs. 10(b), 10(c), 11(b) and 11(c) that maximum value of load effect always plays control role, tail curves of vehicle load effect are close to Weibull distribution and Lognormal distribution. Compared with actual conditions, lognormal distribution is selected as probability distribution model of vehicle load effect in this paper, and its probability density function is as follows

$$f_Y(y) = \frac{1}{\sigma_{\ln Y} y} \varphi\left(\frac{\ln(y) - \mu_{\ln Y}}{\sigma_{\ln Y}}\right) \quad (6)$$

where  $f_Y(y)$  is probability density function of vehicle load effect;  $Y$  represent random variable of vehicle load effect (kN·m);  $\mu_{\ln X1}$  and  $\sigma_{\ln X1}$  are respectively the mean and standard deviation of the natural logarithm of vehicle load effects.

Its cumulative distribution function is given by

$$F_Y(y) = \Phi\left(\frac{\ln(y) - \mu_{\ln Y}}{\sigma_{\ln Y}}\right) \quad (7)$$

Table 4 Countries' regulations for multi-lane transverse reduction factors

Specification/Criterion	Signal lane	Two-lane	Three-lane	Four-lane
U.S. AASHTO	1.00	1.00	0.90	0.75
U.S. AASHTO LRFD	1.20	1.00	0.85	0.65
U.K. BS5400	1.00	1.00	0.78	0.67
U.K. Eurocode	1.00	0.64	0.52	0.46
China JTG D60	—	1.00	0.78	0.67

\*1.2 in Table is counted when multi-lane transverse reduction factors are determined by AASHTO LRFD specifications according to two-lane instead of signal lane; when only one car is on the bridge, it can be heavier than each one of a pair of vehicles and still have the same probability of occurrence, therefore, taking 1.2 conforms to the actual situation

where  $F_Y(y)$  is cumulative distribution function of vehicle load effect;  $\Phi(\cdot)$  is standard normal cumulative distribution function.

According to sample value of vehicle load effect under random vehicle load, maximum likelihood method is adopted to estimate parameters  $\mu_{lnX1}$  and  $\sigma_{lnX1}$  in Eqs. (6)-(7). The estimation results and probability density curve drawn in Eq. (6) are indicated in Figs. 10(b), 10(c), 11(b) and 11(c). It can be seen from Figs. 10(b), 10(c), 11(b) and 11(c), Eq. (6) better describes statistical characteristics of vehicle load effects.

Maximum distribution of vehicle load effect in design reference period is adopted to determine standard value of bridge load. Therefore, the section distribution of vehicle load effect should be converted to the probability distribution of the maximum value in design reference period. Assume period of section distribution is one year, and then probability distribution function of vehicle load effect with 100 year of design reference period  $F_{YT}(y)$  is

$$F_{YT}(y) = [F_Y(y)]^T = [F_Y(y)]^{100} = \left[ \Phi \left( \frac{\ln(y) - \mu_{lnY}}{\sigma_{lnY}} \right) \right]^{100} \quad (8)$$

where  $T$  is design reference period of bridge structure (year).

Its cumulative distribution function is given by

$$f_{YT}(y) = 100 f_Y(y) [F_Y(y)]^{99} = \frac{100}{\sigma_{lnY} y} \varphi \left( \frac{\ln(y) - \mu_{lnY}}{\sigma_{lnY}} \right) \left[ \Phi \left( \frac{\ln(y) - \mu_{lnY}}{\sigma_{lnY}} \right) \right]^{99} \quad (9)$$

## 5. Probability calculation of reduction factors

Since the lane number is different, the load effect is calculated by considering that the most unfavorable loads simultaneously appear. In general, a multi-lane transverse reduction factor is adopted to obtain the load effect.

Table 4 summaries the multi-lane transverse reduction factors in different design codes. It can be found that with the increase of lanes, the probability of vehicle load on all lanes occurred simultaneously at most unfavorable situation

Table 5 Guarantee rate of vehicle load effect during composite girder bridges in design reference period

$L$ , m	One-span bridge			Two-span bridge			
	Two-lane	Three-lane	Four-lane	Two-lane	Three-lane	Four-lane	
10.5	0.8024	0.7213	0.7986	56.1	0.8827	0.8545	0.8476
17.1	0.8352	0.8204	0.7829	69.3	0.9208	0.9352	0.9112
30.3	0.9771	0.9791	0.9783	82.5	0.9200	0.9324	0.9253
42.9	0.9813	0.9801	0.9896	95.7	0.9141	0.8998	0.8872

should be very low.

### 5.1 Calculation methods of reduction factors

Multi-lane transverse reduction factors refer to a multi-lane bridge in the transverse lane. When the vehicle load is not simultaneously, the load effects of the bridge structure should be reduction. Based on probability model of vehicle load effect, multi-lane transverse reduction factors of bridges with different spans should be calculated at this section, in the same exceeding probability with lane load effect. Moreover, the relationship of change rules of multi-lane transverse reduction factors and bridge span was analyzed. It is supposed that  $M_k$  should be lane load effect with different spans calculated when lane load (JTG D60 2015) is loaded to 1/2, 1/3 and 1/4 lanes of bridge structure as shown in Figs. 10(a) and 11(a);  $p$  is probability of vehicle load effect corresponding  $M_k$  when vehicle load is applied to single lane of one- and two-span bridges with different spans and lanes. The result is determined according to Eq. (10) and shown in Table 5. As shown in Table 5, the guarantee rate of vehicle load effects with different spans bridges in design reference period is different. When the bridges span  $L$  is less than 20 m, the guarantee rate of vehicle load effect is smaller, reflecting the sensitivity of small-span bridges for vehicle loads.

$$f_{IT}(y) = 100 f_Y(y) [F_Y(y)]^{99} = \frac{100}{\sigma_{lnY} y} \varphi \left( \frac{\ln(y) - \mu_{lnY}}{\sigma_{lnY}} \right) \left[ \Phi \left( \frac{\ln(y) - \mu_{lnY}}{\sigma_{lnY}} \right) \right]^{99} \quad (10)$$

where  $\mu_{lnY}$  and  $\sigma_{lnY}$  are respectively the mean and standard deviation of the natural logarithm of vehicle load effects when vehicle load is applied to 1/2, 1/3 and 1/4 lanes;  $p$  is guarantee rate of vehicle load effect during design reference period as shown Table 5;  $M_k$  is standard value of lane load effect (kN·m), namely it is section moment of span for corresponding steel beam II in Figs. 10(a) and 11(a).

Moreover, it is supposed that the mid-span section moments of steel girder II for random vehicle loads applied on all lanes, with the PDF  $f_{YT}(y)$ , when they having the same guarantee rate  $p$ , the corresponding load effect is  $M'$ , that is,

$$M' = F_{YT}^{-1}(p), \text{ kN} \cdot \text{m} \quad (11)$$

where  $\mu_{lnY}$  and  $\sigma_{lnY}$  are respectively the mean and standard deviation of the natural logarithm of load effects when vehicle load is applied to 2/2, 3/3 and 4/4 lanes;  $M'$  is the characteristic value of load effects (kN·m) when vehicle load is applied to 2/2, 3/3 and 4/4 lanes and the calculation results are shown in Fig. 12.

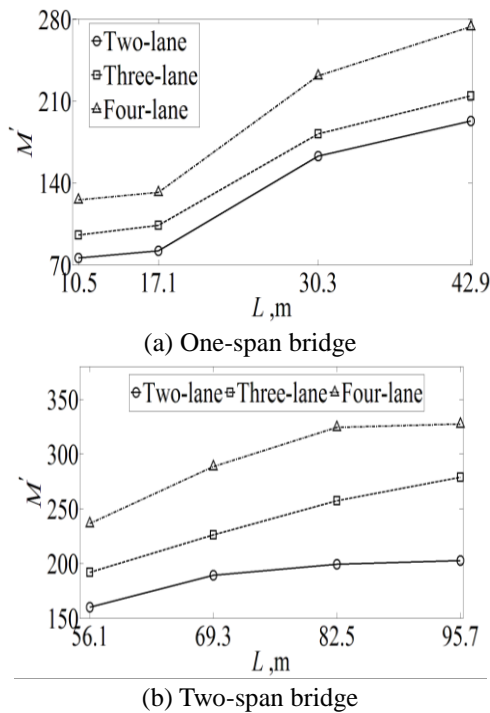


Fig. 12 Characteristic values of vehicle load effect with the same guarantee rate for bridges

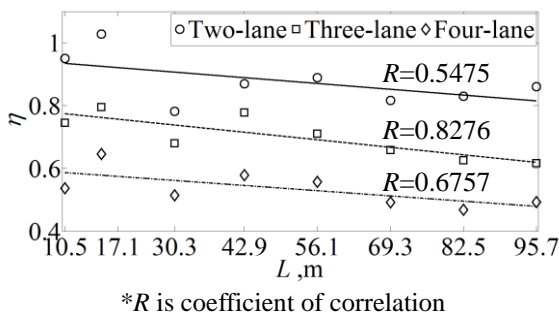


Fig. 13 fitted curves of two-lane, three-lane and four-lane transverse reduction factors

Fig. 12 summaries that standard value of vehicle load effect of one-span and two-span bridge structure under random vehicle loads increases with increase of bridge spans, and the change trend of one-span bridges is larger than that of two-span bridges.

Multi-lane transverse reduction factors are determined by considering the possibility of most unfavorable condition of vehicle load effect by other lanes on bridge deck for specific lanes corresponding standard value of vehicle load effect. Based on the above calculation method, multi-lane transverse reduction factors are acquired as shown in Fig. 13 (scatter plot) by comparison of standard values of load effect between single lane and all lanes, separately applied vehicle load on. Fig. 13 also shows that multi-lane transverse reduction factors decrease with increase of bridge span. By numerical analysis, linear function between multi-lane transverse reduction factors and bridge span can be established.

5.2 Contrastive analysis of reduction factors

Table 6 Comparison of calculation results of two-lane transverse reduction factors in this paper and standard values

Type of bridges	L, m	FEA	AASHTO LRFD*, %	BS5400*, %	Eurocode*, %	JTG D60*, %
One-span	10.5	0.950	-5	-5	33	-5
	17.1	1.027	3	3	38	3
	30.3	0.781	-28	-28	18	-28
	42.9	0.869	-15	-15	26	-15
Two-span	56.1	0.889	-12	-12	28	-12
	69.3	0.816	-23	-23	22	-23
	82.5	0.829	-21	-21	23	-21
	95.7	0.861	-16	-16	26	-16
	Average value of absolute error	0.878	15	15	27	15

\*The specified values of transverse reduction factors in AASHTO LRFD, BS5400, Eurocode and JTG D60 codes are respectively in Table 4

Table 7 Comparison of calculation results of three-lane transverse reduction factors in this paper and standard values

Type of bridges	L, m	FEA	AASHTO LRFD*, %	BS5400*, %	Eurocode*, %	JTG D60*, %
One-span	10.5	0.745	-14	-5	30	-5
	17.1	0.795	-7	2	35	2
	30.3	0.679	-25	-15	23	-15
	42.9	0.778	-9	0	33	0
	56.1	0.711	-20	-10	27	-10
Two-span	69.3	0.658	-29	-19	21	-19
	82.5	0.625	-36	-25	17	-25
	95.7	0.616	-38	-27	16	-27
	Average value of absolute error	0.701	22	13	25	13

\*The specified values of transverse reduction factors in AASHTO LRFD, BS5400, Eurocode and JTG D60 codes are respectively in Table 4

Multi-lane transverse reduction factors calculated according to finite element and probability method, is compared with the standard specification by different countries (Table 4), as shown in Tables 6-8.

Table 6 shows that the range of two-lane transverse reduction factors calculated by the method in this paper is 0.781-1.027 and the average is 0.878, which are approximately closer to specified values by AASHTO LRFD, BS5400 and JTG D60 codes, conversely, relatively greater deviation compared with the values stipulated by Eurocode code. For all two-lane, one- and two-span bridge cases, Eurocode code underestimates the FEA transverse reduction factor by 20% to 40%.

Table 7 shows that the range of three-lane transverse reduction factors calculated by the method in this paper is 0.616-0.795 and the average is 0.701 which are relatively closer to specified values by BS5400 and JTG D60 codes, conversely, relatively greater deviation compared with the values stipulated by AASHTO LRFD and Eurocode codes.

Table 8 Comparison of calculation results of four-lane transverse reduction factors in this paper and standard values

Type of bridges	L, m	FEA	AASHTO LRFD*, %	BS5400*, %	Eurocode*, %	JTG D60*, %
One-span	10.5	0.536	-21	-25	14	-25
	17.1	0.645	-1	-4	29	-4
	30.3	0.514	-26	-30	11	-30
	42.9	0.578	-12	-16	20	-16
Two-span	56.1	0.557	-17	-20	17	-20
	69.3	0.491	-32	-36	6	-36
	82.5	0.468	-39	-43	2	-43
	95.7	0.493	-32	-36	7	-36
Average value of absolute error	0.535	23	26	13	26	

\*The specified values of transverse reduction factors in AASHTO LRFD, BS5400, Eurocode and JTG D60 codes are respectively in Table 4

For all bridge cases, AASHTO LRFD overestimated the FEA transverse reduction factors by 10% to 40%. The Eurocode code underestimates the FEA transverse reduction factors by about 15% to 30%.

Table 8 shows that the range of four-lane transverse reduction factors calculated by the method in this paper is 0.468-0.645 and the average is 0.535. Compared with the specified values by AASHTO LRFD, BS5400, Eurocode and JTG D60 codes, Eurocode code underestimates the FEA transverse reduction factors by 10% to 30% with one lane and various span lengths.

In Tables 6-8, comparison of multi-lane transverse reduction factors calculated by methods in this paper and specified values by other countries is conducted based on actual traffic flow. It can be observed that AASHTO LRFD, BS5400 and JTG D60 codes overestimate FEA transverse reduction factors. While the FEA transverse reduction factors in two-, three-, and four-lane is respectively about 27%, 25% and 13% higher than Eurocode code.

## 6. Conclusions

Based on measured data of vehicle load on main roads in China in recent years, the probability model of random vehicle load was established. Probability model of vehicle load proposed by this paper was respectively loaded to one out of two lane, one out of three lane, one out of four lane, and all lanes of bridge structure, time-varying static load can be conducted. Vehicle load effect of composite girder bridges was confirmed at different arbitrary-time point and under the same guaranteed rate, and then multi-lane transverse reduction factors were calculated. It is significant to consider influence of load mode, number of lane, type of bridges and other factors of vehicle load in analysis. Finally, comparison of multi-lane transverse reduction factors calculated by methods in this paper and specified values by AASHTO LRFD, BS5400, Eurocode and JTG D60 is conducted. The following conclusions are obtained:

- The arbitrary-time point distribution of vehicle load effects can be described by lognormal distribution.

- According to probability theory and FEA method, the calculation method of multi-lane transverse reduction factors is put forward based on random vehicle load; it can be acquired that multi-lane transverse reduction factors of composite girder bridges decrease with increase of bridge span; for the range of multi-lane transverse reduction factors, two-lane is 0.781-1.027, three-lane is 0.616-0.795 and four-lane is 0.468-0.645.

- The values of two-lane transverse reduction factors in AASHTO LRFD, BS5400 and JTG D60 codes are about 15%, 15% and 15% higher than FEA, respectively. The values of three-lane transverse reduction factors in AASHTO LRFD, BS5400 and JTG D60 codes are about 22%, 13% and 13% higher than FEA, respectively. The values of four-lane transverse reduction factors in AASHTO LRFD, BS5400 and JTG D60 codes are about 23%, 26% and 26% higher than FEA, respectively. While for the two-, three-, and four-lane bridges, the Eurocode code underestimated the FEA transverse reduction factors by 27%, 25% and 13%, respectively. The FEA results highlight the importance of span length in determining the transverse reduction factors when designing composite girder bridges with two lanes or more.

## Acknowledgments

The research described in this paper was financially supported by the National Basic Research Program (973 Program Grant No. 2015CB057703) of China.

## References

- AASHTO (2002), *Standard Specifications for Highway Bridges*, 17th Edition, Washington, U.S.A.
- AASHTO LRFD (2012), *American Association of State Highway and Transportation Officials LRFD Bridge Design Specifications*, 7th Edition, Washington, U.S.A.
- Altunişik, A.C., Bayraktar, A. and Sevim, B. (2013), "Analytical and experimental modal analyses of a highway bridge model", *Comput. Concrete*, **12**(4), 377-392.
- Bao, W.G., Li, Y.H. and Zhang, S.D. (1995), "On the reduction coefficients of traffic loading laterally and longitudinally on bridges", *Chin. J. High. Transp.*, **8**(1), 80-86.
- British Standard (2003), *Eurocode 1: Actions on Structures-Part 2: Traffic Loads on Bridges*.
- BS5400 (2006), *Part 2: Specification for Loads*, British Standards Institution, London, U.K.
- Crespo, M.C. and Casas, J.R. (1997), "A comprehensive traffic load model for bridge safety checking", *Struct. Safe.*, **19**(4), 339-359.
- Dawe, P. (2003), *Research Perspectives: Traffic Loading on Highway Bridges*, Thomas Telford, Reston, U.S.A.
- Frederick, G.R. and Tarhini, K.M. (2000), "Wheel load distribution in concrete slab bridges", *Comput. Civil Build. Eng.*, **2000**, 1236-1239.
- Gong, J.X., Yang, X.Y. and He, S.H. (2011), *Research on Load Combination Method and Coefficient*, Rep. Traffic Construction Technical Project of the Western China, CCCC Highway Consultants CO., Ltd, Beijing, China.

- Guo, T., Li, A.Q. and Zhao, D.L. (2008), "Multiple-peaked probabilistic vehicle load model for highway bridge reliability assessment", *J. South. Univ.*, **38**(5), 763-766.
- Helmi, K., Bakht, B. and Mufti, A. (2014), "Accurate measurements of gross vehicle weight through bridge weigh-in-motion: A case study", *J. Civil Struct. Health Monitor.*, **4**(3), 195-208.
- Hołowaty, J. (2012), "Live load distribution for assessment of highway bridges in American and European codes", *Struct. Eng. Int.*, **22**(4), 574-578.
- JTG D60 (2015), *General Code for Design of Highway Bridges and Culverts*, Ministry of Communications, Beijing, China.
- JTG D62 (2004), *Code for Design of Highway Reinforced Concrete and Prestressed Concrete Bridges and Culverts*, Ministry of Communications, Beijing, China.
- Mabsout, M., Tarhini, K. and Jabakhanji, R. (2004), "Wheel load distribution in simply supported concrete slab bridges", *J. Brid. Eng.*, **9**(2), 147-155.
- Mabsout, M.E., Naddaf, I.Y. and Tarhini, K.M. (2002), "Load reduction in steel girder bridges", *Pract. Period. Struct. Des. Constr.*, **7**(1), 37-43.
- Mabsout, M.E., Tarhini, K.M. and Frederick, G.R. (1997), "Finite element analysis of steel girder highway bridges", *J. Brid. Eng.*, **2**(3), 83-87.
- Mabsout, M.E., Tarhini, K.M. and Frederick, G.R. (1999), "Effect of multilanes on wheel load distribution in steel girder bridges", *J. Brid. Eng.*, **4**(2), 99-106.
- Mei, G., Qin, Q. and Lin, D.J. (2004), "Bimodal renewal processes model of highway vehicle loads", *Reliabil. Eng. Syst. Safe.*, **83**(3), 333-339.
- Meski, E.F., Mabsout, M. and Tarhini, K. (2011), "Investigation of AASHTO live-load reduction in reinforced concrete slab bridges", *J. Brid. Eng.*, **16**(6), 792-803.
- Miao, T.J. and Chan, T.H.T. (2002), "Bridge live load models from WIM data", *Eng. Struct.*, **24**(8), 1071-1084.
- Patrick, M.D. and Huo, X.S. (2004), "Finite element modeling of slab-on-beam concrete bridge superstructures", *Comput. Concrete*, **1**(3), 355-369.
- Tarhini, K.M. and Frederick, G.R. (1992), "Wheel load distribution in I-girder highway bridges", *J. Struct. Eng.*, **118**(5), 1285-1294.
- Ting, X.X., Yan, L. and Zhi, W.W. (2015), "Vehicle load spectrum simulation of long-span bridges", *Key Eng. Mater.*, **648**, 35-44.
- Zokaie, T., Imbsen, R.A. and Osterkamp, T.A. (1991), *Distribution of Wheel Loads on Highway Bridges*, National Cooperative Highway Research Program (NCHRP 12-26), Transportation Research Board, Washington, U.S.A.

**Appendix: Conversion to S.I. equivalents**

To convert	To	Multiply by
in	mm	25.4
ft	m	0.305
lb	N	4.448
ksi	MPa	6.895